Progress in Neurocomputing Research

Gerald B. Kang
Editor

ISBN-13: 978-1-60021-863-7
ISBN-10: 1-60021-863-6

www.novapublishers.com

Progress in Neurocomputing Research Kang

Progress in Neurocomputing Research

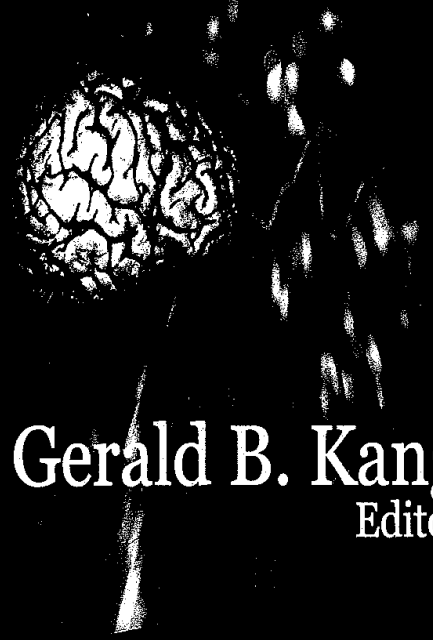

Gerald B. Kang
Editor

Contributors

T. Baidyk
Ángela Blanco
Tak-Wai Chan
Kai-Fu Chan
Frank Emmert-Streib
Daisy Lan Hung
Wen-Jyi Hwang
Jiang-Shing Jiang
E. Kussul
[illegible]a Li
[illegible]uo Lian
[illegible]. Makeyev
Manuel Martín-Merino
Kenji Morita
Mu-Chun Su
Frank van der Velde
Yao-Jung Yeh
Yunong Zhang

Library of Congress Cataloging-in-Publication Data

Progress in neurocomputing / Gerald B. Kang, editor.
p. ; cm.
Includes index.
ISBN-13: 978-1-60021-863-7 (hardcover)
ISBN-10: 1-60021-863-6 (hardcover)
1. Neural networks (Computer science) I. Kang, Gerald B.
QA76.87.P78 2008
006.3'2--dc22

2007030858

Published by Nova Science Publishers, Inc. † New York

CONTENTS

In: Progress in Neurocomputing Research
Editor: Gerald B. Kang, pp. 183-202

ISBN: 978-1-60021-863-7

Chapter 7

A VISUALIZATION MAP THAT AIDS IN DETECTING ACTIVATED REGIONS IN FMRI

Mu-Chun Su[1*], Jiang-Shing Jiang[2], Daisy Lan Hung[3] and Tak-Wai Chan[2]

[1]Department of Computer Science & Information Engineering,
National Central University, Taiwan, R.O.C.
[2]Graduate Institute of Network Learning Technology,
National Central University, Taiwan, R.O.C.
[3]Graduate Institute of Cognitive Neuroscience, National Central University,
Taiwan, R.O.C.

Abstract

A visualization map called V map that can aid in the detection of activated regions in functional magnetic resonance imaging (fMRI) is proposed. The motivation of the V map was attributed to the use of the self-organizing feature map (SOM) as a data clustering tool. Via the visual examination of the map, the user can easily identify activated regions in the fMRI. The proposed visualization map fully utilizes the property of the spatial connectivity of activated pixels, which is an important factor in determining the significance of activated regions in fMRI. The advantage of this technique is that regions of activation can be identified in fMRI without the need of a priori knowledge of expected hemodynamic responses. One artificial data set and one real life data set are used to demonstrate the applicability of the technique.

Keyword: fMRI, self-organizing feature map, clustering algorithm, segmentation, medical imaging

* E-mail address: muchun@csie.ncu.edu.tw

1. Introduction

Functional magnetic resonance imaging (fMRI) is a powerful tool for monitoring regional hemodynamic change following neuronal activations in the brain with high spatial resolution [1]. In a typical fMRI experiment, blocks of baseline and activation images are scanned periodically while the subject is at the "baseline" (e.g., rest) condition and when the subject is performing a specified cognitive or motor task. Two main problems make the detection of activated regions in fMRI difficult: (1) the noisy characteristic of the fMRI data and (2) the variability of the hemodynamic response. Many different approaches have been proposed to analyze fMRI data. These approaches can be dichotomized into two different classes: (1) model-driven approaches and (2) data-driven approaches. The most popular model-driven approaches are the t-test technique and the correlation coefficient analysis (CCA). These two methods share the same disadvantage that we must know the shape and delay of the activation signal (or model function) in advance. Without the a priori knowledge, they are incapable to identify activated regions in fMRI.

In more recent years, data-driven approaches have begun to be employed in analyzing fMRI data [2]-[16]. These approaches do not assess whether the data contain a model function. Popular data-driven approaches include the independent component analysis (ICA) technique and clustering-algorithm-based methods. The ICA technique is a blind source separation method that does not require knowledge of the expected hemodynamic response to detect activated regions in fMRI. It is a method of factoring measured signals into a set of signals that are statistically independent by using a feedforward neural network to estimate the independent components in the data [17]. The crucial problems associated with the ICA technique are the lack of criteria for determining the physiologic importance of each component and the incomplete development and optimization of the method for clinical use. As for the clustering-algorithm-based methods, they group image pixels together based on the similarity of their intensity profile in time (i.e., their time courses) independently of their spatial distribution. Each cluster can be represented by an average time course and output maps can be produced by labeling pixels that belong to the same cluster. Basically, the performance of these methods is greatly dependent on the following factors: (1) the distance measure and (2) the number of clusters. In addition, since most of them cluster pixels independently of their spatial distribution, pixels belonging to the same cluster may be scatted over the image. Therefore, activated regions detected by these clustering-algorithm-based methods are then usually disconnected. This phenomenon contradicts the property of the spatial connectivity which is an important factor in determining the significance of activated regions in fMRI.

In fact, the detection of activated regions in fMRI could also be regarded as a segmentation problem in which the goal is to divide the fMRI data into consistent parts or objects. Hundreds of segmentation techniques have been described in textbooks and other literature. For example, summaries of the techniques can be found in [18]-[20]. Instead of adopting the viewpoint of segmentation to detect activated regions in fMRI, in this study, we propose a visualization map (V map) to analyze fMRI data. Via the proposed V map, activated regions can be visually identified without the need of a priori knowledge of expected hemodynamic responses. The V map can be regarded as a new data-driven approach to analyze fMRI data.

The remaining of the paper is organized as follows. In section 2, we briefly review the background of fMRI data and two widely used analysis techniques. Then the description of the proposed V map is given in section 3. The experimental results are given in section 4. Finally, section 5 concludes the paper.

2. Background

2.1. fMRI Data

Functional magnetic resonance imaging (fMRI) allows assessments of brain activities via local hemodynamic variations over time. In a typical fMRI experiment external stimuli are presented at intervals of several seconds. During an fMRI experiment, images of the brain are acquired while the subject alternates between performing a designed cognitive or motor task and being at rest. Fig. 1 illustrates a typical imaging scenario. The brain is sliced into several (e.g., N_S) slices with a slice thickness of several (e.g., L_{tk}) mm and a slice gap of another several (e.g., L_{gap}) mm, as shown in Fig. 2. That is, a complete brain results in N_s images. After the experiment, a complete scan of the whole experiment will produce N_T images per slice. Therefore, the time course of a pixel at a slice is consisting of N_T time-point long time-series, as shown in Fig. 3.

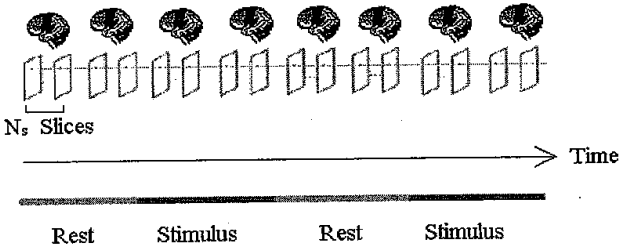

Figure 1. A typical fMRI imaging scenario.

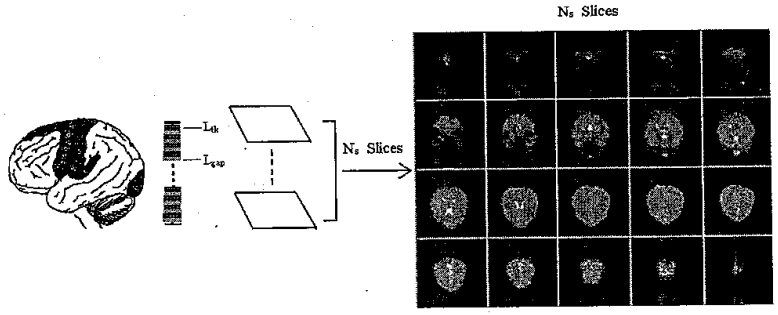

Figure 2. A complete brain is consisted of N_S slices (images).

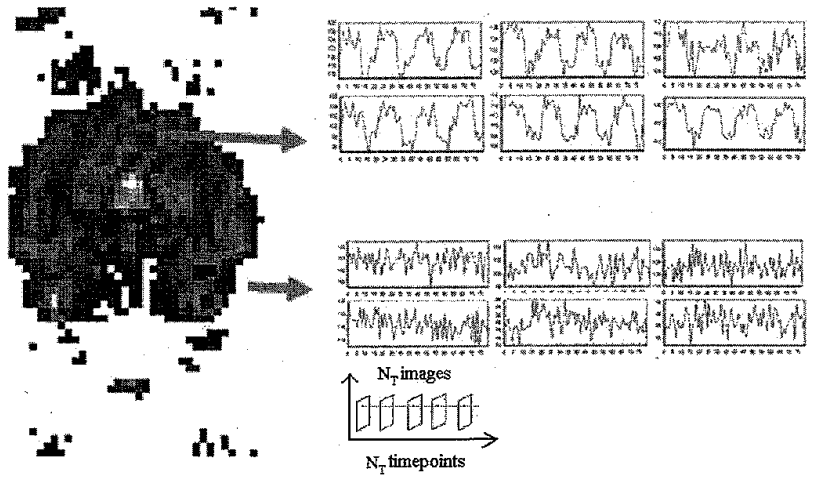

Figure 3. The pixel time courses corresponding to two 2×3 blocks at a particular slice.

Localized signal differences between the resting and activation period are used to reveal the localized neuronal activation associated with the task. The detection of the fMRI response is not a trivial process, because the activation-induced signal changes has a magnitude and time delay determined by an imperfectly understood transfer function of the brain. This transfer function may be characterized by variables dependent on the brain activity and variables independent of brain activity.

2.2. Analyzing Methods

The goal of analyzing fMRI is to detect activated pixels at each slice. Pixels at a slice can be divided into two classes: (1) activated pixels and (2) non-activated pixels. While activated pixels contain pixel time course (or time series) that are related to the stimulus, pixels with no activity correlated to the stimulus are declared to be non-activated pixels. The time series corresponding to non-activated pixels are considered to be background activity.

Currently, the most widely used methods for analyzing fMRI data are based on explicit, priori knowledge regarding the activation time course. The *t*-test technique [21]-[23] and the correlation coefficient analysis (CCA) [24]-[27] are two of the most popular techniques.

The *t*-test assumes that each fMRI time series corresponds to the realization of an identically independent stochastic process and divides the data into two groups, obtained during on (post-stimulus) and off (pre-stimulus) periods. A *t* statistic is calculated by computing the difference of the sample means of each group normalized by the pooled standard deviation. Then activated pixels are detected by using different values of *t* as a threshold. The assumption of the *t*-test is that the measured time-series at each pixel consists of a known activation signal in Gaussian white noise. However, this assumption is not always true in real cases.

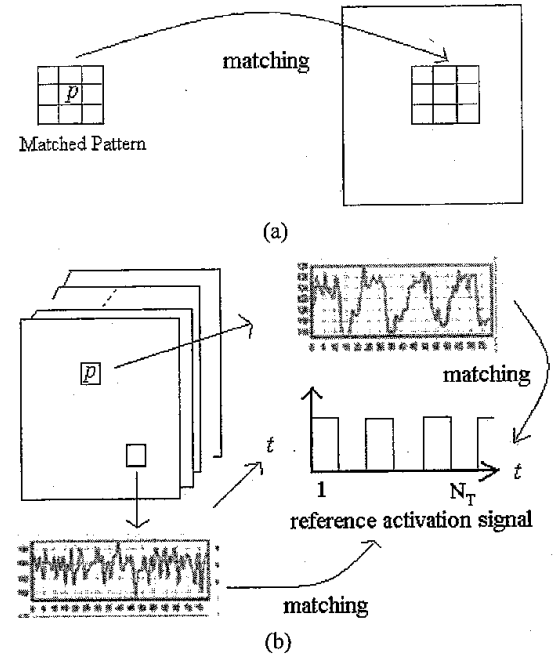

Figure 4. Different matching approaches. (a) the window-based matching in the conventional correlation-based algorithm. (b) the time-course-based matching in the CCA.

In the image segmentation literature, matching is one of the basic approaches to segmentation that it can be used to search specific patterns, to locate known objects in an image, etc. Basically, the idea of correlation-based matching and the CCA, one of the most popular model-based analysis tools in fMRI, share the same idea of the use of matching to search for specific patterns. The major difference between them is as follows. While the conventional correlation-based matching is based on evaluating a match criterion for each location and rotation of a reference pattern in an image, the CCA is based on calculating the correlation between an assumed form of fMRI response (i.e., a boxcar or on/off reference activation signal) and the measured time-series of a pixel in a slice. Fig. 4 can be used to illustrate this kind of difference. After the correlation coefficients have been calculated they are used as a threshold to distinguish between activated pixels and non-activated pixels. Those pixels that show high correlations are declared to be activated pixels. The CCA is successful with simple block-design paradigms in which the neuronal response is assumed to be on/off and the hemodynamic response is known. The main drawback of the CCA is that the correlation coefficients depend on the shape of the reference activation signal (i.e., the hemodynamic response), which is actually unknown. Although a simple boxcar function is usually taken as a reference activation signal, the actual functional response does not resemble a boxcar function and usually differs by subjects, tasks, activated regions, ages, etc. An inaccurate assignment of the reference function usually leads to an incorrect result. In

addition, if differential temporal responses are expected, the performance of the CCA may further degrade.

In more recent years, data-driven approaches have begun to be employed in analyzing fMRI data [2]-[16]. The clustering-algorithm-based approaches play an important role in the data-driven approaches. Clustering algorithms are one of the basic tools for exploring the underlying structure of a given data set. It has been playing an important role in solving many problems such as biology, medicine, society, psychology, pattern recognition, and image processing. The primary objective of cluster analysis is to partition a given data set of multidimensional vectors (patterns) into so-called homogeneous clusters such that patterns within a cluster are more similar to each other than patterns belonging to different clusters. While it is easy to consider the idea of a data cluster on a rather informal basis, it is very difficult to give a formal and universal definition of a cluster. In order to mathematically identify clusters in data, it is usually necessary to first define a measure of distance that will establish a rule for assigning patterns to the domain of a particular cluster center. As it is to be expected, the distance measure is very problem dependent. Different distance measures result in different types of clusters (e.g., compact hyper-spheres, compact hyper-ellipsoids, lines, shells, etc). Cluster seeking is very experiment-oriented in the sense that clustering algorithms that can deal with all situations are not yet available. Extensive and good overview of clustering algorithms can be found in the literature [28]-[32]. There are two major difficulties encountered in clustering data: (1) the presence of large variability in cluster geometric shapes and (2) the number of clusters not always being known *a priori*.

The aim of the clustering-algorithm-based fMRI analyzing approaches is to find a group of pixels that share a similar time course. Therefore, each cluster corresponds to a type of similar activations. The cluster centers are then representative of the types of activations. Subsequently, each pixel can be labeled on the image according to the clustering information. It is then possible to further analyze regions with similar types of activations. Three popular clustering algorithms such as the k-means algorithm [2], [14], fuzzy c-means algorithm [3]-[4], [6], and the self-organizing feature map (SOM) algorithm [9], [11], have been proposed to analyze fMRI data. Due to the high noise level in fMRI data, the clustering results are usually unsatisfactory if the Euclidean distance measure based on the raw time courses is employed. Another problem associated with the k-means algorithm incorporated with the Euclidean distance measure is that the resulting clusters tend to be well-separated hyper-spherical clusters of the same size. The number of activated pixels is usually much smaller than the number of non-activated pixels; therefore, if we use the k-means algorithm with $k = 2$ to cluster fMRI data then it is expected that the activated pixels will be definitely submerged by one of the two large clusters. The two activations corresponding to the two cluster centers won't be correlated to the stimulus patterns. For most of those clustering-algorithm-based approaches usually up to 20 clusters are used. Then all clusters have to be further verified to find whether these clusters can be really categorized as functional activation, acquisition artifact, or just noise.

To improve the clustering results, Golay et al. [33] and Toft et al. [34] proposed to employ a metric based on the correlation between stimulus and time course. However, the use of the stimulus information in calculating the correlations seems to contradict the original goal of the data-driven approach. While the distance metric plays an important role in the clustering results another crucial problem associated with clustering algorithms is the determination of the number of clusters. When the pre-specified number of clusters does not

match the real number of clusters existing in the underlying structure of the data, the clustering result reveals little information and even may end up being totally meaningless. To circumvent the problem, Goutte et al. developed a hierarchical clustering algorithm referred to as the group-average agglomerative method [12]. Another possible solution is to use the SOM algorithm by starting with a sufficient number of nodes. Each node corresponds to a small cluster. Owing to the topology-preserving characteristic which is unavailable in most other clustering algorithms, so-called "superclusters" can be formed by merging neighboring clusters on the SOM map.

In fact, no matter which aforementioned clustering algorithm is employed to cluster fMRI data, it is still possible for pixels belonging to the same cluster to be scattered in the image. As we know, activated pixels should have a tendency of clumping together; therefore, some kinds of post-processing procedures have to be carried out to delete isolated pixels or small-sized connected regions in order to improve the overall performance of detecting activated regions. Recently, some researchers have utilized the property of pixel connectivity into clustering procedures to analyze fMRI data sets [35]-[37].

The most crucial problem associated with the clustering-algorithm-based approaches is the lack of criteria for determining which cluster really corresponds to activated regions. The original goal of the clustering-algorithm-based approaches is to detect activated regions without a prior knowledge of expected hemodynamic responses. If we still need to use the information about the activation paradigm then the original goal is not reached. Unfortunately, these clustering-algorithm-based approaches failed to provide us with a convincing solution to this problem because they either need the information of the stimulus to select the cluster which has the most similar temporal characteristics as the stimulus or they must assume the activated regions exist in which area of the brain so they can identify which cluster corresponds to the activated regions.

3. Method

Based on the aforementioned discussions, we find that these data-driven approaches, to a certain extent, still need the stimulus information. In this study, we propose a visualization map called V map for the detection of activated regions in fMRI. This new analysis tool is really without the use of a priori knowledge of the activation paradigm. The only assumption of the new analysis tool is that activated pixels have a tendency of clumping together. This assumption is physiologically acceptable since the activated regions will be in the spatial vicinity of the neural population concerned with the accomplished task.

The motivation of the V map was attributed to the U-matrix method [38] and the nonlinear projection methods proposed by Kraaijveld et al. [39] and Mao and Jain [40]. These methods are visualization tools to visualize high-dimensional data as a two-dimensional image. These tools share a similar idea. For these tools, the self-organizing feature map (SOM) algorithm [41]-[42] is first used to train a two-dimensional neural network. Then the trained network is to be displayed as an image, whereby every node in the network corresponds to a pixel in the image. The gray value of each pixel is determined by the maximum distance in the feature space of the corresponding node to its

immediate eight neighbors in the network. The larger the distance, the lighter the gray value is. Thus, clusters can be visualized as darker regions with lighter borders.

The original goal of the SOM algorithm is to simultaneously cluster the data set and project those high-dimensional data onto a two-dimensional network structure in a topologically preserving way. In our V map technique, we omit the use of the SOM algorithm. The reasons are twofold. From our viewpoint, an fMR image is already a topologically preserved map since activated pixels will clump together on the image. Therefore, we do not need to employ a nonlinear projection algorithm such as the SOM algorithm to carry out the topologically-preserving projection task. In addition, although the SOM algorithm is claimed to have the topology-preserving characteristic there is no guarantee that a topologically preserved map can be always produced at the end of the training procedure. Therefore, if we expect that we can use the clustering result achieved by the SOM algorithm to produce a topologically preserved labeled map which will then be used to identify the activated regions this expectation may be unrealistic. Based on the twofold considerations we decide to directly process the image and regard each pixel as a separate small cluster.

The whole procedure of generating a V map from a set of fMR images collected from an experiment is presented as follows:

Step 1. Pre-Processing:

First, pixels outside the brain are excluded from the analysis by eliminating those pixels on an fMR image that have signal intensities below a pre-specified threshold. Then the linear baseline drift is removed by use of a regression procedure. In addition, each pixel time course is normalized individually by subtracting its mean and dividing by the variance to be with zero mean and unit variance.

Step 2. Transforming:

For each one of the N_S slices a new image with the same size, which is called a V map, will be generated. Every pixel in the slice has a one-to-one relation to the pixel at the same location in the V map. The gray value of each pixel in the V map is determined by the maximum (or average) correlation coefficient between the corresponding pixel and its eight immediate neighbors in the slice. The larger the maximum or average correlation coefficient, the darker the gray value is. Therefore, darker regions surround by lighter borders in the V map are candidates of activated regions because pixels within the same darker region have similar temporal characteristics corresponding to the accomplished task.

The correlation coefficient between pixels i and j can be computed in either the time-domain space or the frequency-domain space.

Time-domain space

$$cc_t(i,j) = \frac{\sum_{n=1}^{N_T}(x_{in}-\mu_i^t)(x_{jn}-\mu_j^t)}{[\sum_{n=1}^{N_T}(x_{in}-\mu_i^t)^2]^{\frac{1}{2}}[\sum_{n=1}^{N_T}(x_{jn}-\mu_j^t)^2]^{\frac{1}{2}}} \quad (1)$$

where $\underline{x}_i = (x_{i1},\cdots,x_{iN_T})^T$ is the pixel time course for pixel i in the slice, N_T denotes the number of scans, and $\mu_i^t (= \frac{1}{N_T}\sum_{n=1}^{N_T} x_{in})$ represents the average value of the pixel time course for pixel i.

Frequency-domain space

$$cc_f(i,j) = \frac{\sum_{n=1}^{N_f}(f_{in}-\mu_i^f)(f_{jn}-\mu_j^f)}{[\sum_{n=1}^{N_f}(f_{in}-\mu_i^f)^2]^{\frac{1}{2}}[\sum_{n=1}^{N_f}(f_{jn}-\mu_j^f)^2]^{\frac{1}{2}}} \quad (2)$$

where $\underline{f}_i = [f_{i1},\cdots,f_{iN_f}]^T$ is an N_f-dimensional vector consisting of the N_f samples of the magnitude of the Fourier transform of the time course, $\underline{x}_i$, for pixel i, and $\mu_i^f (= \frac{1}{N_f}\sum_{n=1}^{N_f} f_{in})$ represents the average value of the vector $\underline{f}_i$. In the process of Fourier transform the phase information is lost; however, the essential information on the temporal response of the pixel can still be revealed from the magnitude of the Fourier transform.

Basically, the correlation coefficient computed in either the time-domain space or the frequency-domain space can be used to highlight the activated regions. However, we have tended to prefer computing the coefficients in the frequency-domain space because many experimental results demonstrated that the frequency-domain space allowed us with much ease to identify activated regions on the V maps than the time-domain space did. The reason why these two kinds of computations have different performance may be due to the following factors. A common artifact in fMRI is a linear drift of the signal with respect to time, which seems to be resulted from the subject's slight motion during the scanning procedure. Assume that two neighboring pixels have exactly the same shaped time courses but with different time lags. The correlation coefficient between these two pixels is not equal to one any more if it is computed in the time-domain space. Moreover, the fMRI data is usually with noise, the correlation coefficient may be further reduced. The use of the magnitude of the Fourier transform provides us with the ability of being insensitive to time lags because we do not use the phase information in the calculations of the coefficients.

Step 3. Segmenting:

By viewing the map the analyst can detect where the dark regions are located on the V map; however, the precise scopes of the activated regions have to be identified somehow. The scope of a candidate activated region can be determined in either a manual way or an automatic way. In the manual way, one has to move the cursor to point to a candidate pixel to decide whether this pixel should be considered as an activated pixel by comparing its corresponding time course (or the magnitude of the Fourier transform) with the time course (or the magnitude of the Fourier transform) of the nearest darkest pixel. Otherwise, we may

use a thresholding technique to automatically segment the activated regions from the V map. The segmentation task can be easily accomplished if the histogram of the V map presents two obvious peaks; otherwise, correct threshold selection is usually crucial for successful threshold segmentation. Since the histogram of a V map usually is not bi-modal we need to adopt an auxiliary method to segment the V map. First, the pixels with cc values smaller than θ_{cc} are discarded and the range of the gray values of the remaining pixels will then be stretched to be of the range from 0 to 255. Then the threshold selection method proposed by Rider and Calvard [43] is used to determine the optimal threshold to segment the V map into activated regions and non-activated regions. This method assumes that regions of two main gray-levels are present in the image; however, it still works well even if the image histogram is not bi-modal. This method involves four steps and it is iterative, four to ten iterations usually being sufficient. First of all, we assume that the four corners of the image contain background pixels only and the remainder contains object pixels. Second, at time t, compute μ_B^1 and μ_O^1 as the mean background and object gray-level, respectively and set $T^t = (\mu_B^t + \mu_O^t)/2$ as the threshold value. Third, use the threshold value T^t to segment the image to provide an updated background-object distinction. Fourth, if there is no significant difference between the updated threshold and the old threshold then halt; otherwise, return to step 2. The value of the parameter θ_{cc} is determined by the analyst via a scrollbar. To further eliminate some isolated pixels, smooth the contours of connected regions, and eliminate thin protrusions, a morphological operator (e.g., the opening operator) is employed to process the segmented map.

Since good results could be achieved via the automatic way we suggest using the automatic way first. The manual way won't be chosen unless the automatic way cannot achieve reasonable results.

4. Results

To provide a comparison with the proposed V map, we performed the two model-based methods, the t-test technique and the correlation coefficient analysis (CCA), on the same data sets. This included an artificial data set and a real life fMRI data set. The boxcar reference waveform was used in the model-based methods.

For the artificial data set, to assess the performance of each method, receiver operating characteristics (ROC) curves were constructed. The sensitivity or called as true positive ratio (TPR) and the specificity are determined for each step and plotted against the other to generate the ROC curve. For a given threshold the sensitivity is the fraction of all active pixels that actually are classified as active, and the specificity is the proportion of the non-active pixels that are correctly classified as non-active. The false positive ratio (FPR), the fraction of all non-active pixels that are falsely classified as active, equals one minus the specificity. The area under the ROC curve can be used as a measure of the detection performance of a method. The closer the area is to one, the higher the detection accuracy.

To plot the ROC curve for both model-based methods, we varied the threshold of CCA from *cc* = 0.10, 0.15,..., to 0.50, and the threshold of t-test from t value = 0.5, 1.0,..., to 4.0. For our proposed method, we varied the value of θ_{cc} from θ_{cc} = -0.089, -0.049,..., to 0.071.

4.1. Artificial Data Set

We first used the simulated data set generated by Dimitriadou et al. [44] for quantitative performance assessment. This data set is available at *http://www.ci.tuwien.ac.at/research/oenb/oenb_data.html*. It is composed of a time series (35 instances) of a transversal brain slice (128×128 pixels) with a time invariant texture of 4809 pixels (gray/white matter, ventricles) and three regions of activation, two small regions and one large region, (49 pixels, see Figure 5(a)). The signal intensity increases during "activation" in a box-car-like pattern (5 instances off, 5 on, etc). In all activated pixels the related signal increase upon activation was 6%, 5%, and 4% with 3% baseline Gaussian noise of zero mean value added. It resulted in three simulated fMRI data sets with functional CNR (contrast-to-noise ratio) of 2.0, 1.66, and 1.33 respectively.

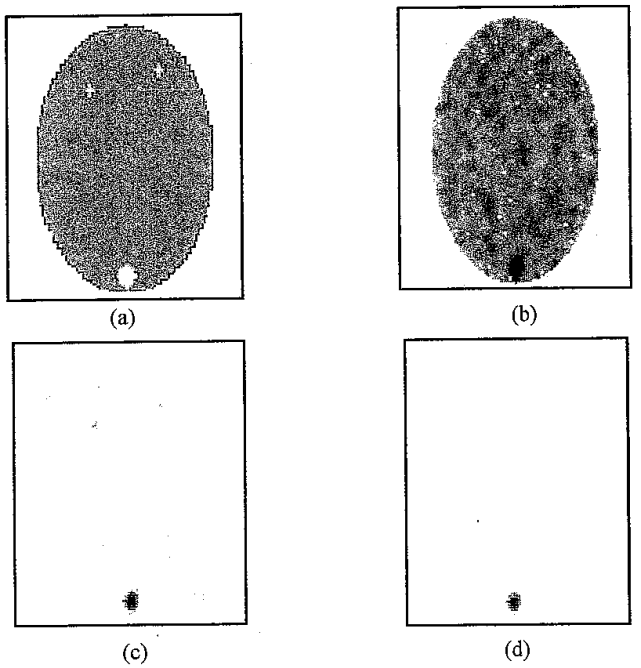

Figure 5. The V maps for the artificial data set. (a) The image in the artificial set. (b) The initial V map. (c) The stretched V map with $\theta_{cc} = 0.031$. (d) The stretched V map with $\theta_{cc} = 0.071$.

Here we use Fig. 5(b)-5(d) to illustrate how the V map can be used to detect the regions of activation. Fig. 5(b) shows the initial V map found by executing the transforming step of the method. One can identify the darkest regions by carefully viewing the initial map. To help the analyst locate the most possible activation regions with ease, two maps whose contrasts have been stretched to the range from 0 to 255 using two different values of θ_{cc} are shown in Fig. 5(c) and 5(d), respectively. By viewing either one of these two figures one may easily identify the activation regions. This example demonstrates that the V map can detect regions of activation without a priori knowledge of expected functional response.

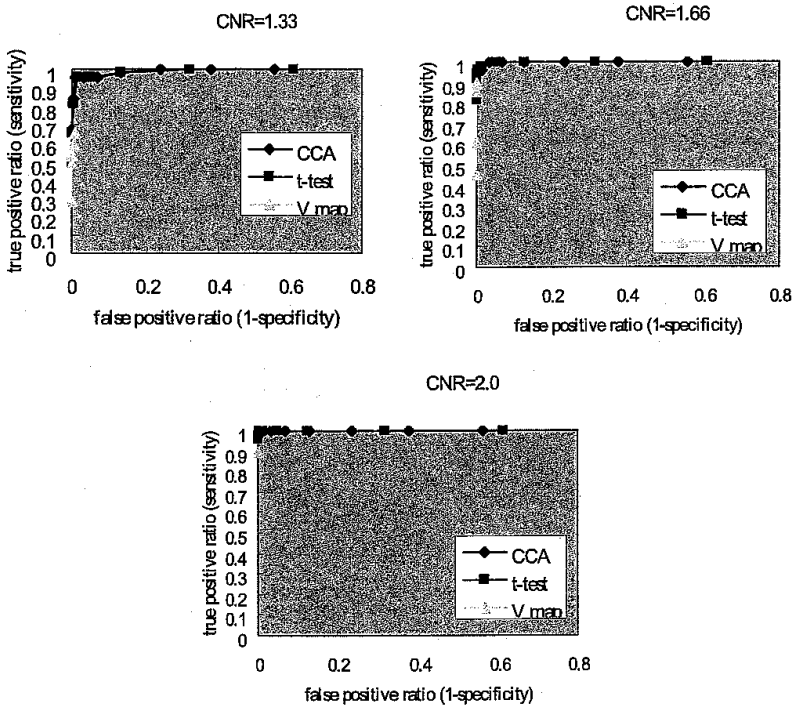

Figure 6. The ROC curve under CNR = (a) 1.33. (b) 1.66. and (c) 2.0.

The ROC analysis of the artificial data set is shown in Fig. 6. While the sensitivities or TPRs of the two model-based methods were superior to the V map when the value of CNR was low, the sensitivities of these three methods reached nearly the same level when CNR = 2.0. By further examining the curves, we may find although the sensitivity reached by the V map decreased as the value of CNR decreased, FPR (i.e., 1 – specificity) was very low and almost fixed. This observation reveals that the V map could correctly identify locations of the activated regions but could not correctly estimate their precise sizes. Figure 7 shows the activation regions and the averaged time-course waveform in the activation regions identified by the V map, the CCA, and the t-test under CNR = 1.33 (Fig. 7(a)) and 2.0 (Fig. 7(b)). By

viewing Fig. 7(a) we find that the largest activation region was detected by all these three methods. While the V map miss-detected the two small activated regions, the CCA, and the t-test still were able to correctly identify the two small regions. These three methods all misclassified some non-activated pixels as activated pixels. The t-test achieved the lowest FPR and the V map had the highest FPR. On the contrary, Fig. 7(b) shows that the V map achieved the lowest FPR among the three methods. In addition, all three activation regions were correctly identified by these methods.

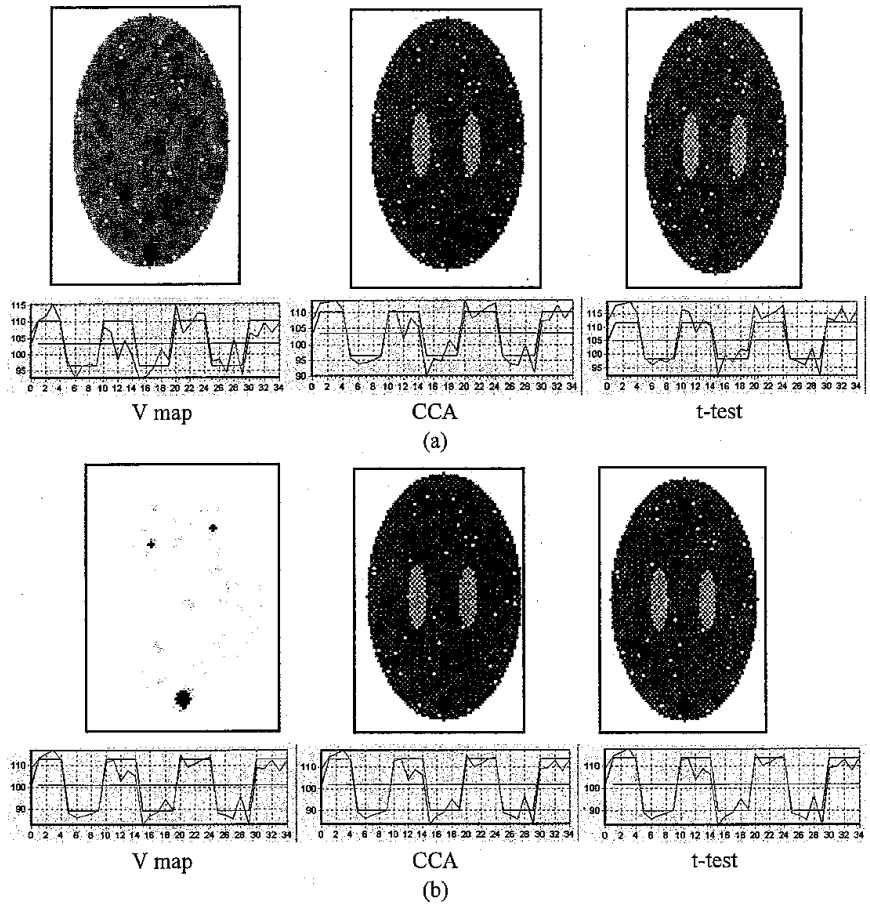

Figure 7. The activation regions and the averaged time-course waveform in the activation regions identified by the V map, the CCA, and t-test under (a) CNR = 1.33 and (b) CNR = 2.0.

4.2. Real Life Data Set

One healthy subject was asked to conduct the following experiment. The subject was asked to alternatively do a visual task and a motor task with total 8 repeated cycles of visual-motor states. Each state consisted of 10 images for each task. For the motor task, the subject was asked to do a rhythmic motion of making a fist and opening with her eyes gazing at the crisscross point shown on the screen. For the visual task, binocular black-and-white checkerboard stimulation was given to the subject at a frequency of 8Hz. The subject did nothing but gazed at the center of checkerboard. This black-and-white checkerboard image was presented with a PC and projected via a LCD projector (Toshiba TY-G3, Japan) outside the shielded room on a screen. The subjects saw the checkerboard image via a homemade reflection mirror.

Imaging was performed on a 3.0-T MedSpec S300 system with a quadrature head coil. The fMRI data were acquired with a T2*-weighted gradient-echo EPI using BOLD contrast (TR/TE/θ = 2000ms/50ms/90°, slice thickness = 5mm, inter-slice interval = 1mm, FOV = 250mm, matrix size = 64×64, slice number = 20, and whole brain covered). For each slice, 80 images were acquired.

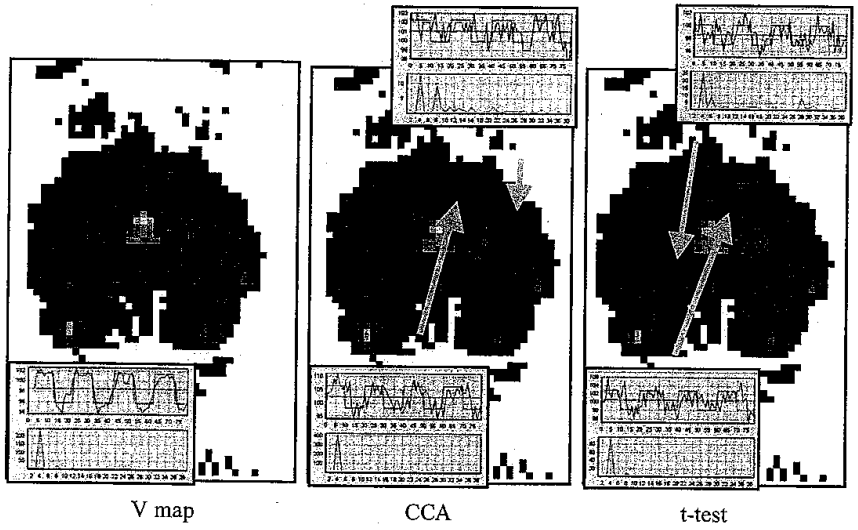

Figure 8. The activated regions on the visual cortex.

For the experiment, activated regions detected by the V map, (θ_{cc} = 0.115 for the 7th slice and θ_{cc} = -0.268 for the 16th slice), CCA ($p<0.001$, corresponding $CC>0.358$), and t-test ($p<0.001$, two tailed, corresponding t-value>3.21) are shown in Fig. 8 (slice 7) and Fig. 9 (slice 16). Basically, all these three methods could successfully identify the activated regions on the visual cortex (Fig. 8) and primary motor cortex (Fig. 9). Since the ground truth is

however unknown it is difficult to make any numerical comparisons regarding the detection performance. However, we still can find that CCA and the t-test did erroneously identify many unrelated pixels. After further examining Fig. 8 and Fig. 9 we find that activated regions detected by CCA and t-test were activated by at least two kinds of signal sources. The large activated regions were due to the actual experimental paradigm and some detected regions were outside the visual cortex or the motor cortex (a possible location of cortical venous vessels). On the contrary, the V map performed very well on the detection of activated region in the visual cortex. One thing should be mentioned is that the V map detected three activated regions in the 16th slice shown in Fig.9. Two regions were on the primary motor cortex and the smallest one was near the motor cortex. The frequency analysis of this region indicates it contained two peaks. One peak corresponded to two times of the frequency component of the actual experimental paradigm and the other one corresponded to one half of the frequency component of the actual experimental paradigm. The physical basis for this observation is not well understood. It deserves to be further inspected.

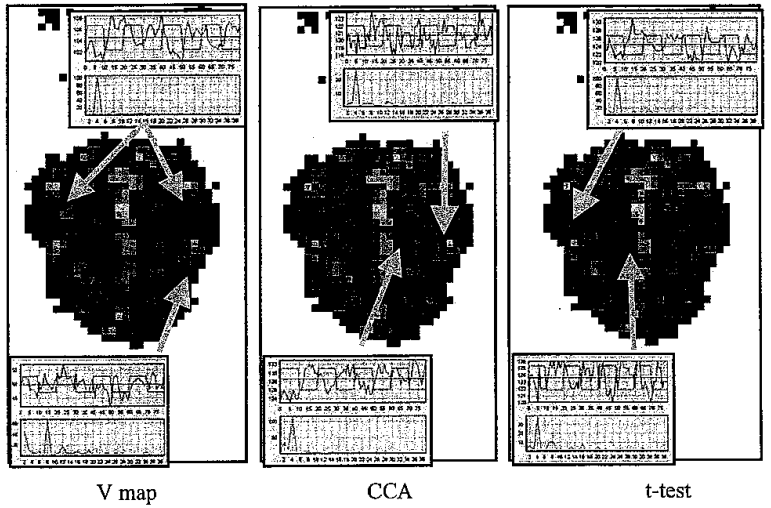

Figure 9. The activated regions on the primary motor cortex.

5. Discussions

In order to investigate the role played by the window size we used a larger window size (e.g., 5×5 window size) to re-run the two data sets. The results are shown in Fig. 10. Apparently, both window sizes, 3×3 and 5×5, could detect the same activation regions whose sizes are large enough. For the case of the artificial data set in CNR = 1.33, we find that the two small untruly activation regions, shown in Fig. 7(a), were not miss-detected by the 5×5 window size. For the activation regions detected in the primary motor cortex we find that the small region on the right bottom corner of Fig. 9 was not declared to be activated

by the 5×5 window size. Based on these observations, some remarks can be made. First, large window size won't increase the false positive ratio. Second, large window size may decrease the true positive ratio if activation regions are not large enough. It is due to the fact that the average correlations within a large window size will be decrease if only a small fraction of pixels within the large window size are truly correlated with each other. This results in the decrease of the discrimination between activated regions and non-activated regions. Therefore, a large window size may decrease the false positive ratio at the price of being unable to detect small activation regions.

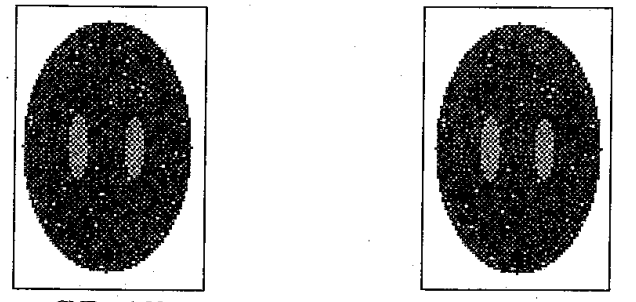

Figure 10. The activation regions by the V map using a 5×5 window size under (a) the artificial data set and (b) real life data set.

From the limited experimental results conducted on one artificial data set and one real life data set, we found that model-based methods could achieve more acceptable performance (e.g., higher sensitivity) than the V map did even when the noise level was high. This observation is not surprising because model-based methods fully utilize the information of the functional response model but the V map doesn't use any a priori information. Although the V map is not able to estimate the precise sizes of the activated regions it can correctly find the locations of the activated regions even though the noise level is high. In addition, the V map

may find some "interesting" regions within which pixels have similar reaction patterns even if these reaction patterns are not similar to the functional response pattern. These regions found by the V map deserve to be further inspected by experts to reveal unexpected information from them.

6. Conclusion

In this paper, the V map technique has been presented and validated. The only assumption for the V map is that in general not a single pixel will be activated by a specified cognitive or motor task, rather groups of tens to hundreds of pixels. It presents several originalities with respect to several conventional analysis methods. The performance of the V map is demonstrated by the simulation results on an artificial data set and a real life data set. Compared to model-based methods, our V map can efficiently detect regions of activation in fMRI without a priori knowledge of expected hemodynamic responses. Compared with current clustering-algorithm-based methods, the V map offers several appealing properties: 1) the processing time involved with clustering algorithms is no longer needed; 2) the determination of the optimal cluster number is not a problem any more; and 3) the order of data and the random initialization of the cluster centers are not a problem any more. In fact, many researchers had pointed out that most clustering approaches make assumptions about cluster shape and size so that the algorithms might artificially induce a geometrical structure that deviates from the real structure of the data. Then this might result in misinterpretations of the analysis results [11], [44]-[46]. Fortunately, the V map does not have such a problem. In addition, the V map is capable of detecting regions within which pixels have similar activation patterns that may be different to the real model function. If these un-expected activation regions can be further inspected more information may be revealed.

The method does have its limitations. If the activation region is very small and/or the noise level is very high then our method may fail. In addition, the V map cannot predict the precise sizes of the activated regions though it can point out the right locations. Finally, no matter which analysis method (of course including the V map), the region declared to be activated still needs to be further inspected and confirmed by the corresponding experts based on the knowledge of the stimulus paradigm.

Acknowledgement

This work was partly supported by the National Science Council under the NSC-95-2221-E-008-128, the NSC-95-2524-S-008-001, and the NSC-95-2752-E-008-002-PAE, and the Ministry of Economic Affairs under the 95-EC-17-A-02-S1- 029.

References

[1] S. Ogawa, T. M. Lee, A. R. Kay, and D. W. Tank, Brain magnetic resonance imaging with contrast dependent on blood oxygenation. *Proc Natl Acad Sci USA*, 87, 9868–9872 (1990).

[2] X. Ding, T. Masaryk, P. Ruggieri, and J. Tkach, Analysis of time-course functional MRI data with clustering method without use of reference signal. *Proc., SMR, 2nd Annual Meeting*, San Francisco, 630 (1994).

[3] G. Scarth, M. McIntrye, B. Wowk, and R. L. Somorjai, Detection of novelty in functional images using fuzzy clustering. *Proc., SMR, 3rd Annual Meeting*, Nice, 238 (1995).

[4] G. Scarth, E. Moser, R. Baumgartner, M. Alexander, and R. L. Somorjai, Paradigm free fuzzy clustering-detected activations in fMRI: a case study. *Proc., SMR, 4th Annual Meeting,* New York, 1784 (1996).

[5] X. Ding, T. Masaryk, P. Ruggieri, and J. Tkach, Detection of activation patterns in dynamic functional MRI with a clustering technique. *Proc., SMR, 4th Annual Meeting*, New York, 1798 (1996).

[6] X. Golay, S. Kollias, D. Meier, and P. Boesinger, Optimization of a fuzzy clustering technique and comparison with conventional post processing methods in fMRI. *Proc., SMR, 4th Annual Meeting*, New York, 1787 (1996).

[7] H. Fischer and J. Hennig, Clustering of functional MR data. *Proc., SMR, 4th Annual Meeting*, New York, 1779 (1996).

[8] M. J. McKeown, S. Makeig, G. G. Brown, T.-P. Jung, S. S. Kindermann, A. J. Bell, and T. J. Sejnowski, Analysis of fMRI data by blind separation into independent spatial components. *Hum Brain Mapp*, 6(3), 160-88 (1998).

[9] H. Fischer and J. Henning, Neural network-based analysis of MR time series. *Magn Reson Med.*, 41, 124-131 (1999).

[10] A. Baune, F. T. Sommer, M. Erb, D. Wildgruber, B. Kardatzki, G. Palm, and W. Grodd, Dynamical cluster analysis of cortical fMRI activation. *NeuroImage*, 9, 477-489 (1999).

[11] S. C. Ngan and X. Hu, Analysis of functional magnetic resonance imaging data using self-organizing mapping with spatial connectivity. *Magn Reson Med.*, 41, 939-946 (1999).

[12] C. Goutte, P. Toft, E. Rostrup, F. A. Nielsen, and L. K. Hansen, On clustering fMRI time series. *NeuroImage*, 9, 298-310 (1999).

[13] M. J. Fadili, S. Ruan, D. Bloyet, and B. Mazoyer, Unsupervised fuzzy clustering analysis of fMRI time series. *Human Brain Mapping*, 10, 160–178 (2000).

[14] C. Baudelet and B. Gallez, Cluster analysis of BOLD fMRI time series in tumors to study the heterogeneity of hemodynamic response to treatment. *Magn Reson Med.*, 49(6), 985-90 (2003).

[15] M. Quigley, V. Haughton, J. Carew, D. Cordes, C. Moritz, K. Arfanakis, and M. E. Meyerand, Comparison of independent component analysis and conventional hypothesis-driven analysis for clinical functional MR image processing. *AJNR Am. J. Neuradiology*, 23, 49-58 (2002).

[16] B. Whitcher, A. J. Schwarz, H. Barjat, S. C. Smart, R. I. Grundy, and M. F. James, Wavelet-based cluster analysis: data-driven grouping of voxel time-courses with application to perfusion-weighted and pharmacological MRI of the rat brain. *NeuroImage*, 24, 281-295 (2005).

[17] J. B. Anthony and J. S. Terrence, An information-maximization approach to blind separation and blind deconvolution, *Neural Computation*, 7, 1129-1159, (1995).

[18] R. M. Haralick and L. G. Shapiro, Survey: image segmentation techniques, Computer. *Vision Graphics Image Processing*, 29, 100-132 (1985).

[19] P. K. Sahoo, S. Soltani, A. K. C. Wong, and Y. C. Chen, A survey of thresholding techniques, Computer. *Vision Graphics Image Processing*, 41, 233-260 (1988).

[20] N. R. Pal and S. K. Pal, A review on image segmentation techniques, *Pattern Recognition*, 26, 1277-1294 (1993).

[21] R. E. Walpole and R. H. Myers, *Probability and statistics for engineers and scientists,* 4th ed., Macmillan Publishing Co., New York.

[22] R. T. Constable, G. McCarthy, T. Allison, A. W. Anderson, and J. C. Gore, Functional brain imaging at 1.5 T using conventional gradient echo MR imaging technique, *Magn. Reson. Imaging*, 11, 451-459 (1993).

[23] N. Lange and S. L. Zeger, Non-linear Fourier time series analysis for human brain mapping by functional magnetic resonance imaging. *Applied Statistics,* 46, 1-29 (1997).

[24] P. A. Bandettini, E. C. Wong, R. S. Hinks, R. S. Tikofsky, and J. S. Hyde, Time course EPI of human brain function during task activation, *Magn. Reson. Med,* 25, 390-397 (1992).

[25] P. A. Bandettini, A. Jesmanowicz, E. C. Wong, and J. S. Hyde, Processing strategies for time-course data sets in functional MRI of the human brain, *Magn. Reson. Med*, 30, 161-173 (1993).

[26] O. Friman, J. Cedefamn, M. Borga, P. Lundberg, and H. Knutsson, Detection of neural activity in fMRI using canonical correlation analysis, *Magnetic Resonance in Medicine*, 45, 323-330 (2001).

[27] O. Friman, M. Borga, P. Lundberg, and H. Knutsson, Exploratory fMRI analysis by autocorrelation maximization, *NeuroImage*, 16, 386-395 (2002).

[28] A. K. Jain and R. C. Dubes, *Algorithms for Clustering Data,* Englewood Cliffs, NJ: Prentice Hall, New Jersey (1988).

[29] R. O. Duda and P. E. Hart, *Pattern Classification and Scene Analysis*, New York: Wiley (1973).

[30] J. Bezdek, *Pattern Recognition with Fuzzy Objective Function Algorithms*. New York: Plenum (1981).

[31] J. Hartigan, *Clustering Algorithms*, New York: Wiley (1975).

[32] J. Tou and R. Gonzalez, *Pattern Recognition Principles*. Reading, MA: Addison-Wesley (1974).

[33] X. Golay, S. Kollias, G. Stoll, D. Meier, A. Valavanis, and P. Boesiger, Fuzzy membership vs. probability in cross correlation based fuzzy clustering on fMRI data. In Third International Conference on Functional Mapping of the Human Brain. *NeuroImage*, 3, S481(1997).

[34] P. Toft, L. K. Hansen, F. A. Nielsen, C. Goutte, S. Strother, N. Lange, N. Morch, C. Svarer, O. B. Paulson, R. Savoy, B. Rosen, E. Rostrup, and P. Born, On clustering of fMRI time series. In Third International Conference on Functional Mapping of the Human Brain. *NeuroImage*, 3, S456 (1997).

[35] S. D. Forman, J. D. Cohen, M. Fitzgerald, W. F. Eddy, M. A. Mintun, and D. Noll, Improved assessment of significant activation in functional magnetic resonance imaging (fMRI): use of a cluster-size threshold. *Magn Reson Med*,3, 636-647 (1995).

[36] J. Xiong, J. H. Gai, J. L. Lancaster, and P. T. Fox, Clustered pixels analysis for functional MRI activation studies of the human brain. *Hum Brain mapping*, 3, 287-301 (1995).

[37] K. J. Friston, K. J. Worsley, R. S. J. Frackowiak, J. C. Mazziotta, and A. C. Evans, Assessing the significance of focal activation using their special extent. *Hum Brain mapping*, 1, 210-220 (1994).

[38] A. Ultsh and H. P. Siemon, Kohonen's self organizing feature maps for exploratory data analysis, *Proceedings of International Neural Networks Conference*, 305-308 (1990).

[39] M. Kraaijveld, A. J. Mao, and A. K. Jain, A nonlinear projection method based on Kohonen's topology preserving maps, *IEEE Trans. on Neural Networks*, 6, 548-559 (1995).

[40] J. Mao and A. K. Jain, Artificial neural networks for feature extraction and multivariate data projection, *IEEE Trans. on Neural Networks*, 6, 296-317 (1995).

[41] T. Kohonen, *Self-Organization and Associative Memory*, 3rd ed. New York, Berlin: Springer-Verlag, 1989.

[42] T. Kohonen, *Self-Organizing Maps*, Berlin, Germany: Springer-Verlag, 1995.

[43] T. W. Ridler and S. Calvard, Picture thresholding using an iterative selection method. *IEEE Transactions on Systems, Man, and Cybernetics*, 8, 630-632 (1978).

[44] D. Evgenia, B. Markus, W. Christian, H. Kurt, and M. Ewald, A quantitative comparison of functional MRI cluster analysis. *Artificial Intelligence in Medicine*, 1-35 (2003).

[45] E. Dimitriadou, A. Weingessel, and K. Nornik, A combination scheme for fuzzy clustering, *International Journal of pattern recognition and artificial intelligence*, 16, 901-912 (2002).

[46] C. Goutte, L. K. Hansen, M. G. Liptrot, and E. Rostrup, *Feature-space clustering for fMRI meta-analysis, human Brain mapping*, 13, 165-183 (2001).

In: Progress in Neurocomputing Research
Editor: Gerald B. Kang, pp. 203-222

ISBN: 978-1-60021-863-7

Chapter 8

FPGA IMPLEMENTATION OF COMPETITIVE LEARNING WITH PARTIAL DISTANCE SEARCH IN THE WAVELET DOMAIN

Wen-Jyi Hwang, Hui-Ya Li, Yao-Jung Yeh and Kai-Fu Chan
Department of Computer Science and Information Engineering,
National Taiwan Normal University, Taipei, 117, Taiwan

Abstract

This chapter presents a novel algorithm for the field programmable gate array (FPGA) realization of the competitive learning (CL) algorithm with k-winners-take-all activation. The k winning neurons for updating are those best matching the input vector in the wavelet domain with partial distance search (PDS). In most applications, the PDS is adopted as a software approach for attaining moderate codeword search acceleration. In this chapter, a novel PDS algorithm well-suited for hardware realization is proposed. The algorithm employs subspace search, finite precision calculation and multiple-coefficient accumulation techniques for the effective reduction of the area complexity and computation latency. A novel sorting architecture is also proposed for identifying the k winning neurons after the PDS process.

The proposed implementation has been adopted as a custom logic block in the arithmetic logic unit (ALU) of the softcore NIOS processor. The custom instructions are also derived for accessing the custom logic block. The CPU time of the NIOS processor executing the PDS program with the custom instructions for k-winners-take-all CL training is measured. Experiment results show that the CPU time is lower than that of Pentium IV processors executing the PDS programs without the support of custom hardware.

1. Introduction

Data clustering is useful in several exploratory pattern analysis, grouping, decision making and machine learning situations, including data mining, document retrieval, pattern classification, image segmentation and data compression. In artificial neural networks (ANNs)[Haykin, 1998], clustering is commonly realized by competitive learning (CL) techniques [Grossberg, 1987; Kohonen, 1990], where the neurons of the network compete